Reversing an extracellular electron transfer pathway for electrode-driven NADH generation

Nicholas M. Tefft[1] and Michaela A. TerAvest[1]*

[1]Department of Biochemistry and Molecular Biology, Michigan State University, East Lansing, MI, USA
*corresponding author
Address: 603 Wilson Rd., East Lansing, MI, 48823 Email: teraves2@msu.edu

Abstract

Microbial electrosynthesis is an emerging technology with the potential to simultaneously store renewably generated energy, fix carbon dioxide, and produce high-value organic compounds. However, limited understanding of the route of electrons into the cell remains an obstacle to developing a robust microbial electrosynthesis platform. To address this challenge, we engineered an inward electron transfer pathway in *Shewanella oneidensis* MR-1. The pathway uses native Mtr proteins to transfer electrons from an electrode to the inner membrane quinone pool. Subsequently, electrons are transferred from quinones to NAD^+ by native NADH dehydrogenases. This reverse functioning of NADH dehydrogenases is thermodynamically unfavorable, therefore we have added a light-driven proton pump (proteorhodopsin) to generate proton-motive force to drive this activity. Finally, we use reduction of acetoin to 2,3-butanediol via a heterologous butanediol dehydrogenase (Bdh) as an electron sink. Bdh is an NADH-dependent enzyme, therefore, observation of acetoin reduction supports our hypothesis that cathodic electrons are transferred to intracellular NAD^+. Multiple lines of evidence indicate proper functioning of the engineered electrosynthesis system: electron flux from the cathode is influenced by both light and acetoin availability; and 2,3-butanediol production is highest when both light and a poised electrode are present. Using a hydrogenase-deficient *S. oneidensis* background strain resulted in a stronger correlation between electron transfer and 2,3-butanediol production, suggesting that hydrogen production is an off-target electron sink in the wild-type

29 background. This system represents a promising genetically engineered microbial
30 electrosynthesis platform and will enable a new focus on synthesis of specific compounds using
31 electrical energy.

32 **Introduction**

33 Microbial electrosynthesis is a technology that utilizes microbes for production of useful
34 chemicals using carbon dioxide, water, and electricity as feedstocks (1). While most microbial
35 electrosynthesis efforts to date have targeted fuel production, other possible applications include
36 production of platform chemicals or bioplastics (2). With pressure to develop sustainable
37 production systems, microbial electrosynthesis is an attractive technology to simultaneously
38 produce valuable products and store electricity generated by wind and solar technologies. Initial
39 efforts have focused on three primary platforms for microbial electrosynthesis: pure cultures of
40 acetogens (3, 4); undefined mixed cultures (5, 6); and electron shuttles paired with model
41 bacterial strains (7, 8). While these approaches have demonstrated proof-of-concept, significant
42 improvements in product yield and product spectrum are necessary to make microbial
43 electrosynthesis economically viable.

44 Pure culture microbial electrosynthesis systems have been developed in an effort to
45 understand the mechanism of electron uptake from a cathode. These systems primarily utilize
46 acetogenic bacteria because they are naturally capable of converting carbon dioxide into acetate
47 using hydrogen or other inorganic electron donors (9, 10). Multiple reports show that acetogens
48 are capable of using an electrode in place of native electron donors (3, 4). While acetate is a
49 relatively low value product, genetic modification may yield strains capable of producing other
50 compounds through electrosynthesis (11). While this is a promising approach, significant
51 challenges to acetogen engineering remain, and further developments are necessary (11, 12). An

alternative approach that may yield specific products is to utilize chemical electron mediators to transfer electrons from an electrode into existing model organisms. This approach has been successful in multiple organisms to generate products such as succinate and ethanol (7, 13–15). However, the cost of the mediator and downstream separations likely make this approach too costly for industrial scale up.

Mixed culture approaches to microbial electrosynthesis have also borne success, due to their ability to generate a range of products without genetic modification. Early efforts in this area have primarily generated acetate, with adjustments to operating conditions driving increased yield (16–18). However, other molecules can also be produced, including butyrate, butanol, and ethanol (5, 19). Selective enrichment of the community is important to improve yields and product specificity (6, 17). While evidence that higher value products are attainable increases the attractiveness of electrosynthesis using undefined mixed cultures, off-target production remains problematic. For example, increased abundance of methanogens over time has posed difficulties for long term experiments due to decreased acetate titers and increased methane production (6, 20). Further, a mixed community cannot be engineered to produce a specific high-value compound with any current technology.

Overall, optimization of existing approaches to microbial electrosynthesis has been hampered by poorly defined interactions between bacteria and cathode electrodes. In most cases, the mechanism of electron transfer is unknown, although in mixed culture systems, H_2 is recognized as a major electron carrier between the electrode and microbes (5). For pure cultures, direct electron transfer has been proposed, but not proven (3, 4). Similarly, specific mechanisms of electron transfer via chemical mediators are only beginning to be investigated (13). In contrast, transmembrane electron transfer is much better understood between dissimilatory metal

reducing bacteria and anode electrodes. *Shewanella oneidensis* MR-1 is particularly well understood and the structure of the Mtr pathway and its function in transferring electrons to the outer surface of the cell have been thoroughly described in the last two decades (21–28).

The well understood electron transfer mechanism of *Shewanella* makes it an excellent candidate to engineer a microbial electrosynthesis system from the ground up using synthetic biology tools. Initial steps to explore the use of *S. oneidensis* MR-1 for microbial electrosynthesis have demonstrated reverse electron transfer through the Mtr pathway. Ross et al. (29) showed electron transfer from a cathode to *S. oneidensis* MR-1 with fumarate as an electron sink, indicating that the Mtr pathway can transfer electrons from a cathode to respiratory quinones. More recent work by Rowe et al. (30) has demonstrated that *S. oneidensis* MR-1 can also catalyze electron transfer from a cathode to oxygen through the Mtr pathway and the quinone pool.

While previous work has demonstrated the ability to generate reduced quinones via a cathode, this is not sufficient to power intracellular reduction reactions. Electrons in the quinone pool have too positive a redox potential to be spontaneously transferred to NAD^+ (ca. -80 mV_{SHE} for menaquinone:menaquinol vs. ca. -320 mV for NAD^+:NADH) and have only been transferred to electron acceptors with a more positive redox potential, such as fumarate (ca. +30 mV_{SHE}). Electrons should ideally be transferred to an intracellular, lower potential electron carrier to be useful for electrosynthesis. NADH is a promising intracellular electron carrier to target because it is involved in many metabolic reactions and is relatively accessible from the quinone pool through NADH dehydrogenases. Under typical conditions, NADH dehydrogenases catalyze the favorable transfer of electrons from NADH to quinones and conserve energy as a proton-motive force (31). However, NADH dehydrogenases may also catalyze the reverse redox reaction,

98 utilizing proton-motive force as an energy source, as observed in purple photosynthetic bacteria
99 (32).

100 Based on previous work and our knowledge of *S. oneidensis* MR-1 metabolism, we
101 hypothesized that NADH dehydrogenases could be driven in reverse to transfer electrode-
102 derived electrons into the cell. Therefore, we engineered a system relying on the native Mtr
103 pathway and NADH dehydrogenases to catalyze the electron transfer steps and using a
104 heterologous light-driven proton pump to generate proton motive force (PMF) to drive NADH
105 dehydrogenases in reverse (**Figure 1**). We expressed butanediol dehydrogenase and provided its
106 substrate, acetoin, to provide an electron sink and a mechanism to track NADH generation. This
107 system represents a generalizable platform to use cathodes to drive NADH-dependent reductions
108 in *S. oneidensis* MR-1. Further development of this platform could lead to a new capability to
109 generate specific, high-value compounds using electricity and carbon dioxide as feedstocks.
110

111 **Results and Discussion**

112 Development of modified *S. oneidensis* strains

113 Genes encoding proteorhodopsin (PR) and butanediol dehydrogenase (Bdh) were cloned into a
114 medium copy plasmid with a constitutive promoter and conjugated into *S. oneidensis* (both WT
115 and a strain lacking hydrogenases; Δ*hyaB*Δ*hydA*) (**Table 1**). A FLAG tag was added to the C-
116 terminus of each protein to facilitate detection by Western blot. Both proteins were detectable in
117 cleared lysates using an anti-FLAG antibody, confirming successful expression (**Figure S1**). To
118 confirm function of Bdh, the modified strain was grown aerobically in the presence of 15 mM
119 exogenous acetoin in LB. Accumulation of 2,3-butanediol was observed by HPLC, indicating

that the expressed Bdh is functional (**Figure S2**). Function of PR expressed from a similar plasmid was previously demonstrated in *S. oneidensis* MR-1 (33, 34).

Light and current drive a target reduction reaction in modified *S. oneidensis*

To determine the capability of the engineered cells to accept electrons from a cathode, the strain lacking hydrogenases and carrying a plasmid with PR and Bdh was pre-grown and inoculated into bioelectrochemical systems at a final density of $OD_{600} = 0.17$. This mutant strain was used to ensure that H_2 did not act as a mediator between cells and the electrode. This mutant was previously shown to lack the ability to produce or consume H_2 (35, 36). To minimize the influence of organic carbon as an electron donor, the bioelectrochemical systems initially contained oxygen (ambient) and the working electrode was set at an anodic potential (+0.4 V_{SHE}). This was done to decrease the availability of organic carbon by oxidizing stored organic material and media components carried over during inoculation. After 6 hours, the working electrode was switched to a cathodic potential (-0.3 V_{SHE}), and N_2 sparging was used to remove oxygen from the bioreactors. Each bioelectrochemical system was equipped with green LED lights around the working electrode chamber to drive proton pumping by PR (**Figure S3**). After switching to the working electrode to a cathodic potential, a stable cathodic current between -5 and -8 µA was observed. After 16 hours, an anoxic acetoin solution was injected into each bioreactor to a final concentration of 10 mM. After acetoin injection, an increase of -12 to -18 µA was observed in all bioelectrochemical systems (**Figure 2**). Note that for cathodic current, a greater negative current represents a greater amount of electron transfer.

To determine the influence of proton pumping on electron uptake, we compared cells with and without functional PR by pre-growing the strain with or without the essential PR

cofactor, all-*trans*-retinal. We refer to PR with retinal as holo-PR and PR without retinal as apo-PR. Cathodic current was significantly higher, ($p=0.03$) in systems with holo-PR (**Figure 3**). We confirmed that the increased current was due to PR activity by turning off the LED lights attached to the bioreactor. When the lights were turned off, cathodic current generated by cells with holo-PR decreased, while cells with apo-PR were unaffected (**Figure 3**). This supports the model that the effect of light is dependent on functional PR; if the effect of light was due to heating or interaction of light with native components, we would expect cells with apo-PR to have a similar response to cells with holo-PR. The dependence of current on holo-PR and light supports our hypothesis that enhanced PMF generation by PR promotes electron uptake by the modified strain.

During the same experiment, we also measured 2,3-butanediol accumulation to determine whether cathodic electrons were directed toward the target reaction, acetoin reduction. As with current, 2,3-butanediol accumulation was greater in the bioelectrochemical systems with holo-PR (**Figure 4**). Based on the total charge transfer over the course of 6 days, accumulation of 0.17 ± 0.02 mM 2,3-butanediol was expected by the end of the experiment. Accumulation of 0.19 ± 0.01 mM 2,3-butanediol was actually observed. The experiment was repeated using the same conditions, with the exception that the electrode was disconnected from the potentiostat. This experiment confirmed that acetoin reduction was driven by the electrode (**Figure 4**). Indeed, 2,3-butanediol production was significantly reduced when the electrode was not poised ($p=0.01$), and accumulation of only 0.13 ± 0.00 mM was observed. Based on our observations, 0.06 mM of the 2,3-butanediol (32% of total production) was generated through the electrode-dependent process. We hypothesize that 2,3-butanediol was not completely eliminated when the electrode was not poised because remaining organic carbon from the inoculum could be oxidized to generate the

166 NADH needed for acetoin reduction. Although we attempted to remove as much organic carbon
167 from the experiment as possible, some cells may have lysed during the washing and inoculation
168 process, thus providing organics to the surviving cells.

169 To determine whether acetoin reduction (as an electron sink) was necessary for inward
170 electron transfer, we also performed experiments with strains lacking *bdh*. When Bdh was not
171 expressed, no 2,3-butanediol was detectable in the bioreactors after 6 days, and cathodic current
172 was significantly reduced, ($p=0.02$). The strain without Bdh generated ca. -11 μA when holo-PR
173 was present (**Figure 5**), representing a ca. 32% reduction in electron transfer compared to the
174 strain with Bdh. This indicates that full activity of the inward electron transfer system is
175 dependent on acetoin reduction, although there is also some Bdh-independent electron transfer.
176 This experiment also allows us to refine our comparisons between charge transfer and 2,3-
177 butanediol accumulation. By subtracting the total charge transfer catalyzed by the strain without
178 Bdh from the strain with Bdh, we can calculate the amount of charge transfer that is Bdh-
179 dependent. We calculate that 0.03 mM of 2,3-butanediol accumulation is expected based on the
180 amount of Bdh-dependent electron transfer. This amount of charge transfer agrees well with the
181 0.06 mM of electrode-dependent 2,3-butanediol accumulation that we observed.

182 Electron uptake by the strain without Bdh was light-dependent when holo-PR was
183 present, indicating that the Bdh-independent process requires PMF generation. This may indicate
184 that the Bdh-independent process also relies on reverse activity of NADH dehydrogenases,
185 although we do not yet know the eventual fate of electrons transferred to the cells without Bdh.
186 No other typical metabolic byproducts of *S. oneidensis* MR-1 (e.g., acetate, formate) were
187 detectable by our HPLC analysis.
188

189 Hydrogen is an electron sink for inward electron transfer

190 A common question in previous work on microbial electrosynthesis is whether H_2 mediates
191 electron transfer, because it can be produced abiotically at the cathode (37). Because small
192 amounts of hydrogen are difficult to measure and may be scavenged quickly by cells on the
193 electrode, it has been challenging to rule out hydrogen as a mediator. We have attempted to do so
194 using an approach similar to Deutzmann et al. (38), i.e., by using a hydrogenase mutant strain.
195 The strain we used does not have the ability to use molecular hydrogen as an electron source or
196 sink (35, 36, 39). To determine whether a hydrogen mediated pathway would function when
197 hydrogenases were present, we also performed the experiments described above in a wild-type
198 background. (Note: these experiments were performed without the initial oxic/anodic step, see
199 Methods for details.) When hydrogenase activity was present, overall current increased while
200 2,3-butanediol accumulation decreased (**Figure 6**). This indicates that rather than acting as a
201 mediator, H_2 was an electron sink for *S. oneidensis* on the cathode. If hydrogen acted as a
202 mediator in this system, we would expect a simultaneous increase in both current and 2,3-
203 butanediol when hydrogenases were present. Our results indicate that cells with hydrogenases
204 generated H_2 and that when the pathway to hydrogen was cut off, electrons were directed more
205 efficiently toward acetoin reduction.
206
207 Comparison with previous work
208 Our results represent an advance in the field of microbial electrosynthesis because we have
209 engineered a pathway to generate intracellular reducing power with a detailed understanding of
210 the electron transfer mechanism. The transmembrane electron conduit connecting the quinol pool
211 to electrodes has been very well characterized (21–23, 28, 40) and is known to be reversible (29,

212 41). We hypothesized that we could take inward electron transfer in *S. oneidensis* MR-1 one step
213 further by utilizing PMF to overcome the thermodynamic barrier of the quinol:NAD^+ reduction
214 and an excess of electron sink (Bdh/acetoin) to avoid over reduction of the NAD^+:NADH pool.
215 The results presented here support that hypothesis; we have shown that electron transfer to the
216 target reaction is dependent on the electrode and on each of the modifications made to the strain.
217 Further, the target reaction is NADH-dependent, indicating that we have successfully connected
218 the electrode to the intracellular NADH pool.

219 While the system described here is one of the best understood inward electron transfer
220 demonstrations to date, there is still more to learn. One critical knowledge gap is exactly how
221 electrons are transferred from the quinol pool to NADH. The *S. oneidensis* MR-1 genome
222 encodes four NADH:quinone oxidoreductases and any of them could be involved in inward
223 electron transfer (42, 43). However, because we have observed dependence of inward electron
224 transfer on PMF, we hypothesize that the proton-coupled NADH dehydrogenase, Nuo, is a major
225 contributor to inward electron transfer. Future studies with Nuo deletion strains will enable us to
226 elucidate the link between respiratory quinones and NADH in our system.

227 In this study, we have successfully driven a heterologous reduction reaction inside living
228 bacteria using an extracellular electrode as the electron source. Rather than using native
229 capabilities of acetogenic bacteria, we engineered a metal-reducing organism to reverse the flow
230 of electrons in its respiratory chain. This represents a proof of concept for an engineered
231 microbial electrosynthesis pathway, and with further development this platform can be used to
232 upgrade bioproducts through electrofermentation or to fix CO_2. Because electrical energy is one
233 of the inputs to the system, the organic molecules produced also represent storage of electrical
234 energy. This type of storage strategy will become essential as wind and solar power capacity

235 increase. Wind and solar energy are intermittent sources; therefore, robust energy storage
236 methods are critical. While significant improvements in engineered microbial electrosynthesis
237 must still be made, a critical mass of researchers forming around this concept will help propel
238 *Shewanella* based electrosynthesis toward real world application.
239
240 **Methods**
241 *Bacterial strains, plasmids, and growth conditions*
242 Strains and plasmids used in this study are listed in Table 1. *E. coli* strains were grown at 37°C
243 and *S. oneidensis* strains at 30°C, both with shaking at 250 rpm. Strains were grown in LB
244 medium (Miller, Accumedia) for assembly and initial verification of strains. Strains bearing
245 pBBR1-MCS2-derived plasmids were grown with a final concentration of 50 μg/mL kanamycin.
246 Pre-cultures for bioelectrochemical experiments were grown in M5 minimal medium: 1.29 mM
247 K_2HPO_4, 1.65 mM KH_2PO_4, 7.87 mM NaCl, 1.70 mM NH_4SO_4, 475 μM $MgSO_4 \cdot 7H_2O$, 10 mM
248 HEPES, 0.01% (w/v) casamino acids, 1X Wolfe's mineral solution (Al was not included), and
249 1X Wolfe's vitamin solution (riboflavin was not included), pH adjusted to 7.2 with 5 M NaOH.
250 M5 medium was supplemented with D,L-lactate to a final concentration of 20 mM. M5 medium
251 with the following modifications was used in the working electrode chamber during
252 bioelectrochemical experiments: 100 mM HEPES, no carbon source, no casamino acids, 1 μM
253 riboflavin.
254
255 *Design and assembly of Bdh and Bdh-PR plasmids*
256 The gene sequence encoding butanediol dehydrogenase in *Enterobacter cloacae* was
257 downloaded from the NCBI gene database (NCBI Reference NC_014121.1). The codon usage

was optimized for *S. oneidensis* MR-1 using JCAT Codon Adaptation Tool (www.jcat.de). A FLAG tag (44) was added immediately before the stop codon and the Salis lab RBS calculator (45) was used to design an optimized RBS for the Bdh-FLAG sequence. Sequences of 20 base pairs flanking the target SmaI restriction sites in the pBBR1-MCS2 sequence were added as flanking regions on the codon optimized RBS-Bdh-FLAG sequence for use in assembly. The entire sequence was submitted to Integrated DNA Technologies for synthesis as a gBlock gene fragment. The same general procedure was utilized to add the gene coding for proteorhodopsin to the plasmid containing *bdh*.

We isolated pBBR1-MCS2 plasmid DNA from *E. coli* using an E.Z.N.A plasmid DNA kit (Omega Bio-Tek). Prepared plasmid DNA was linearized using SmaI (New England Biolabs, Ipswich, MA) digestion for 4 hours at 25°C. The synthesized RBS-Bdh-FLAG insert was resuspended in water to a final concentration of 10 ng/µL and was assembled with linearized pBBR1-MCS2 plasmid using NEBuilder High Fidelity DNA assembly kit (New England Biolabs) using 50 ng of pBBR1-MCS2 and 100 ng of RBS-Bdh-FLAG insert. Assembled pBBR1-MCS2-Bdh was transformed into *E. coli* Mach1 chemically competent cells (Invitrogen). pBBR1-MCS2-Bdh-PR was prepared as above except pBBR1MCS2-Bdh was digested using NdeI and SpeI (New England Biolabs, Ipswich, MA) for 3 hours at 37°C prior to assembly with the synthesized PR gene. Transformants were initially screened via PCR using M13 forward and reverse primers and then sequenced (Sanger sequencing, RTSF Genomics Core, Michigan State University) to verify proper assembly and transformation. Verified Bdh and Bdh-PR plasmids were transformed into chemically competent *E. coli* WM3064 for use in conjugation with *S. oneidensis*. Conjugation was performed using a standard protocol for *S. oneidensis* MR-1 (46).

Verifying expression by Western blot

Expression of Bdh and PR were verified via Western blot through use of FLAG tags added during gene synthesis. Cells were cultured in 5 mL of LB for 16 hours before 200 µL was centrifuged for 2 minutes at 10,000 rpm. Supernatant was removed, and cells were resuspended in 200 µL of a mixture of 1 mL Laemmli buffer, 20 µL of concentrated bromophenol blue (JT Baker, D29303) in 5X Laemmli buffer, and 10 µL of 1 M DTT. Cells were vortexed to mix and incubated at 95°C for 10 minutes. A mini-PROTEAN tetra cell electrophoresis chamber (Biorad, 1658005EDU) was loaded with 1X TGS buffer. Samples were vortexed a 5 µL was loaded onto a mini-protean TGX stain free gel (Biorad, 4568095) alongside 5 µL of Precision Plus ladder (Biorad, 1610376).

Samples were run at 100 V for 1.5 hours until dye front moved off the gel. The gel cassette was broken, and gel removed to 1X Transfer buffer (Biorad, 10026938). Proteins were then transferred to a nitrocellulose membrane (Biorad, 1704270) using a Biorad Turbo transfer system (Biorad, 1704150). The membrane was rinsed with 30 mL TBST buffer, this buffer was discarded, and the membrane was blocked using 50 mL of 3% BSA TBST buffer for 1 hour on an orbital shaker. Blocking solution was discarded and replaced with 30 mL of 3% BSA TBST buffer then 7.8 µL of 3.85 mg/mL anti-FLAG antibody (Sigma-Aldrich, F3165) was added. The membrane was then incubated for 16 hours at 4°C, on an orbital shaker.

The membrane was then rinsed for 5 minutes with TBST buffer three times. After rinsing 30 mL of 3% BSA TBST buffer with 0.0625 µL of anti-mouse antibody (Sigma-Aldrich, A9044) was added. The membrane was incubated for 1 hour at RT. Buffer was discarded and the membrane rinsed with TBST buffer for 5 minutes, three times. ECL Clarity chemiluminescence solution (Biorad, 1705061) was prepared by mixing 10 mL of peroxide solution with 10 mL of

304 enhancer solution, then adding the entire volume to the membrane. The membrane was incubated
305 for 5 minutes, the ECL solution was discarded and the membrane was imaged using a Kodak
306 4000R image station and Caresteam Molecular Imaging software.
307
308 *Bioelectrochemical system construction and operation*
309 Bioelectrochemical measurements were performed in custom two-chambered bioreactors
310 separated by a cation exchange membrane (Membranes International, CMI-7000S) cut in a 4.5
311 cm circle, to completely cover the 15 mm opening connecting working and counter chambers.
312 Working electrodes were prepared from carbon felt (Alfa Aesar, 43200RF) cut into 50x25 mm
313 rectangles and adhered to a titanium wire using carbon adhesive (Sigma-Aldrich, 09929-30G)
314 and allowed to dry for 16 hours. Reference electrodes were prepared by oxidizing silver wires
315 electrochemically in a dilute KCl solution and fixing them in saturated KCl-agar in a custom-
316 made glass housing. The housing maintained ionic connection between the reference electrode
317 and working chamber via a magnesia frit (Sigma-Aldrich, 31408-1EA). Counter electrodes were
318 graphite rods 1/8" in diameter (Electron Microscopy Science, 07200) suspended in the counter
319 chamber filled with PBS. Working chambers were filled with 140 mL of M5 medium (100 mM
320 HEPES, no Casamino acids) prior to autoclaving. After autoclaving, 1.7 mL 100X vitamin stock,
321 1.7 mL Wolfe's minerals (no Al), 0.17 mL 50 mg/mL kanamycin, and 0.85 mL 0.2 mM
322 riboflavin were added to working chamber.
323 Reactors were connected to a potentiostat (VMP, BioLogic USA) and the working
324 electrode poised at +0.4 V_{SHE}. Current was measured every 1 second for the duration of the
325 experiment. Current measurements were collected for at least 16 hours prior to inoculation.
326 Reactors were inoculated with cultures grown in 50 mL M5 medium supplemented with 20 mM

D,L-lactate. Cultures were grown in 250-mL flasks at 30°C for 17 hours shaking at 275 rpm. After 17 hours, 25 µL 20 mM all-*trans*-retinal (vitamin A aldehyde, Sigma-Aldrich, R2500), the essential proteorhodopsin cofactor (47), was added to designated flasks for functional PR testing to a final concentration of 10 µM and all flasks were returned to incubator, shaking, for 1 hour.

To achieve higher inoculum density without adjusting growth time and phase, two 50 mL culture volumes were prepared for each reactor. Absorbance at 600 nm was determined for each culture using a biophotomer (Eppendorf, D30) before the volume was transferred to a 50 mL conical tube (VWR, 89039-664) and centrifuged for 5 minutes at 10,000 rpm (Thermo Scientific ST8R; Rotor: 75005709). Supernatant was removed, and a second volume of cells was added to the conical tube containing the cell pellet before a second centrifugation step. Supernatant was removed, and the combined pellets were resuspended in 10 mL of M5 (100 mM HEPES).

Absorbance at 600 nm was determined for each prepared volume of cells before being standardized to OD_{600}=3.6. The working chamber of each bioelectrochemical system was then inoculated with 9 mL of standardized cell suspension using an 18g needle (Beckton Dickson, 305196) and 10-mL syringe (Beckton Dickson, 302995). The working electrode was poised at +0.4 V_{SHE} for 6 hours, in the presence of ambient oxygen before the potential was changed to -0.3 V_{SHE}, and N_2 gas, 99.9% (Airgas) was bubbled into the reactors through a 0.2 µm filter. The rate of flow of nitrogen gas was observed using a bubbler attached to the gas outlet line from the reactors. The rate of gas flow was maintained so there was positive pressure against the water in the bubbler and bubble rate was kept constant between reactors. After 16 hours, sterile, anoxic acetoin solution was added to a final concentration of 10 mM.

Prior to inoculation, 0.93 m of green LED light strips (FAVOLCANO, 600 LEDs/5 m, 24 W/5 m, ≤6A /5 m) were attached to the exterior of the working chamber and switched on. Light

cycling was performed at 24 hours post acetoin injection, lights were turned off for 1 hour followed by 1 hour on. Light cycles at 24 hours were repeated three times, after which lights were left on.

Samples were regularly removed from the bioreactors for determination of OD_{600} and HPLC analysis. A 2-mL sample was taken approximately every 24 hours using a 21g needle (Beckton Dickson, 305167) and 3-mL syringe (Beckton Dickson, 309657). One mL was used for determination of OD_{600}. One mL was transferred to a micro-centrifuge tube (VWR, 20170-038) and frozen at -20°C until preparation for HPLC analysis. Experiments without a set potential on the working electrode were set up as above except, immediately after acetoin injection the potentiostat was disconnected from the working electrodes.

Experiments testing for the effect of hydrogenase activity (**Figure 6**) were performed as above expect as follows. Potential was set to -0.3 V_{SHE} during background data collection and no anodic potential was used. Oxygen removal using N_2 gas was also started during background data collection and continued for the entire experiment. Cultures grown for reactor inoculation were standardized to the lowest observed OD_{600} after 18 hours of growth, instead of a target OD of 3.6. Finally, acetoin was injected two hours after inoculation once a stable base line current was achieved.

HPLC Analysis

HPLC analysis was performed on a Shimadzu 20A HPLC, using an Aminex HPX-87H (BioRad, Hercules, CA) column with a Micro-guard Cation H^+ guard column (BioRad, Hercules, CA) at 65°C. Compounds of interest were separated using a 0.6 mL/min flow rate, in 5 mM sulfuric acid with a 30-minute run time. Eluent was prepared by diluting a 50% HPLC-grade sulfuric acid

373 solution (Fluka) in Milli-Q water and degassing the solution at 37°C for 3-5 days before use.
374 Compounds of interest were detected by a refractive index detector (Shimadzu, RID-20A)
375 maintained at 60°C. Samples were prepared by centrifuging 1-mL samples taken from the
376 working electrode chambers for 10 minutes at 13,000 rpm in a microcentrifuge (Minispin Plus,
377 Eppendorf) to remove cells. The supernatant was removed and transferred to a 2.0-mL glass
378 HPLC vial (Vial: Restek, 21140; Cap: JG Finneran, 5395F09). Mixed standards of 2,3-
379 butanediol and acetoin were prepared at concentrations of 1, 2, 5, 10, and 15 mM. Samples were
380 maintained at 10°C by an auto-sampler (Shimadzu, SIL-20AHT) throughout analysis. Acetoin
381 and 2,3-butanediol concentrations in the samples were determined using linear calibration curves
382 based on the external standards.
383
384 *Data analysis*
385 Analysis of HPLC and current data was performed using Rstudio using the following packages:
386 ggplot2 (48), reshape2 (49), dplyr (50), and TTR (51).
387
388 **Acknowledgements**
389 The authors thank Dr. Jeffrey Gralnick (University of Minnesota) for providing a plasmid
390 containing the PR gene and Dr. N. Cecilia Martinez Gomez for helpful comments on the
391 manuscript. This work was partially funded by NSF CAREER award 1750785. This work was
392 also supported by the USDA National Institute of Food and Agriculture, Hatch project 1009805.
393

Tables and Figures

Table 1. Strains and plasmids used in this study

Strain or plasmid	Description	Source
E. coli		
Mach1	Host strain for plasmids	
WM3064	Conjugation strain for *S. oneidensis*	(52)
S. oneidensis		(53)
MR-1	Wild Type	
Δ*hyaB*Δ*hydA*	Hydrogenase double knockout mutant	(54)(55)
Plasmids		
pBBR1-MCS2	Kan resistance, broad host vector	(56)
pBBR1-PR	pBBR1MCS2 bearing proteorhodopsin from uncultured marine gamma proteobacterium *Prochlorococcus marinus* GenBank accession #: AF279106_37	(57)(33)
pBdh	pBBR1MCS2 bearing butanediol dehydrogenase gene from *Enterobacter cloacae*	This study
pBdh-PR	pBBR1MCS2 bearing butanediol dehydrogenase from *Enterobacter cloacae* and proteorhodopsin from uncultured marine gamma proteobacterium *Prochlorococcus marinus* GenBank accession #: AF279106_37	This study

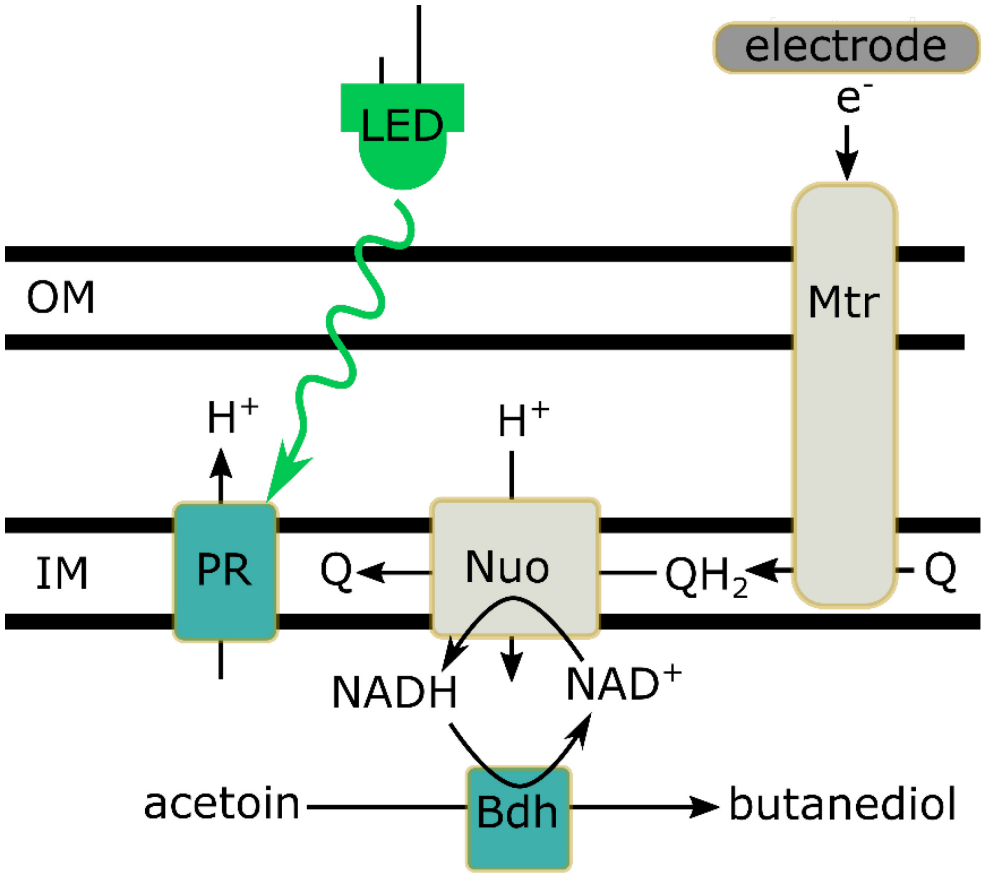

Figure 1. Engineered inward electron transfer pathway. *Shewanella oneidensis* MR-1 pathway designed to transfer electrons from the electrode to NAD^+ to generate intracellular reducing equivalents. Native proteins are shown in grey, heterologous proteins are shown in green. OM: outer membrane; IM: inner membrane; LED: green light source. Nuo is one of four NADH dehydrogenases encoded in the *S. oneidensis* MR-1 genome.

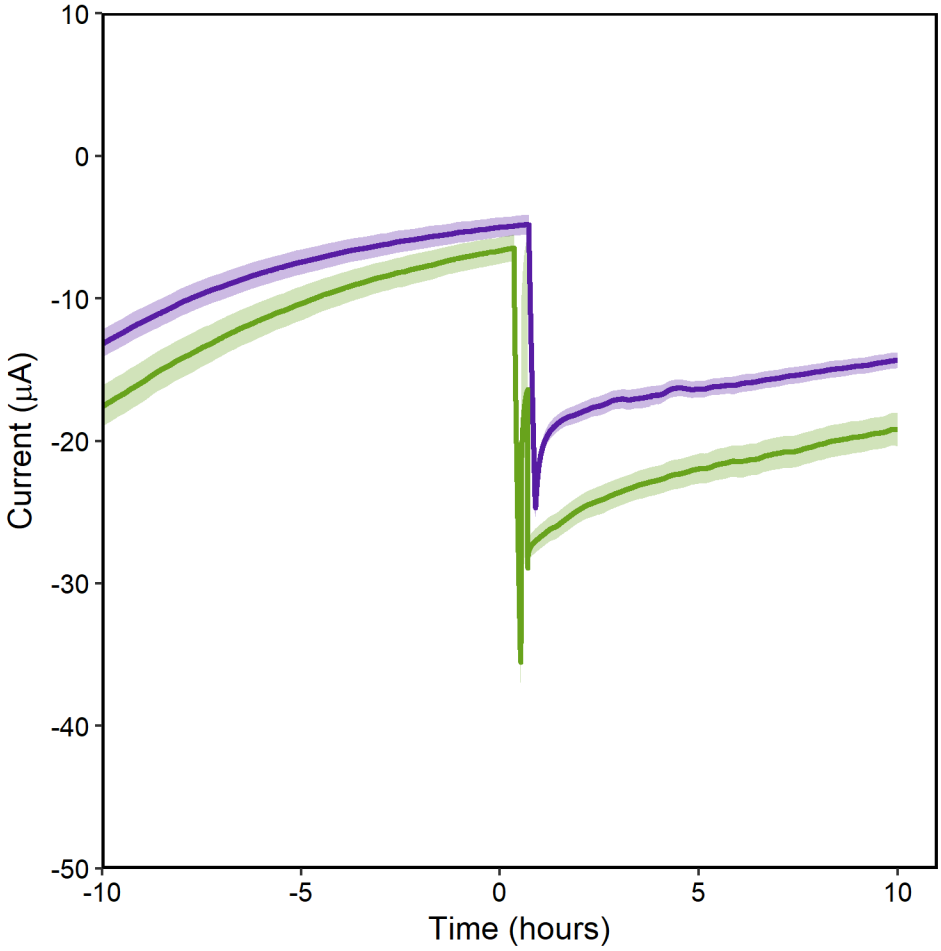

406
407 **Figure 2. Cathodic current measurement during electron acceptor injection.** Cathodic
408 current increases significantly after the electron acceptor, acetoin, is added to the
409 bioelectrochemical system. Time 0 represents acetoin injection. Current measured in
410 bioelectrochemical systems containing cells grown with holo-PR are shown in green and those
411 containing apo-PR are shown in purple. Each line represents the average of three replicates with
412 standard error shown in transparent ribbons.
413

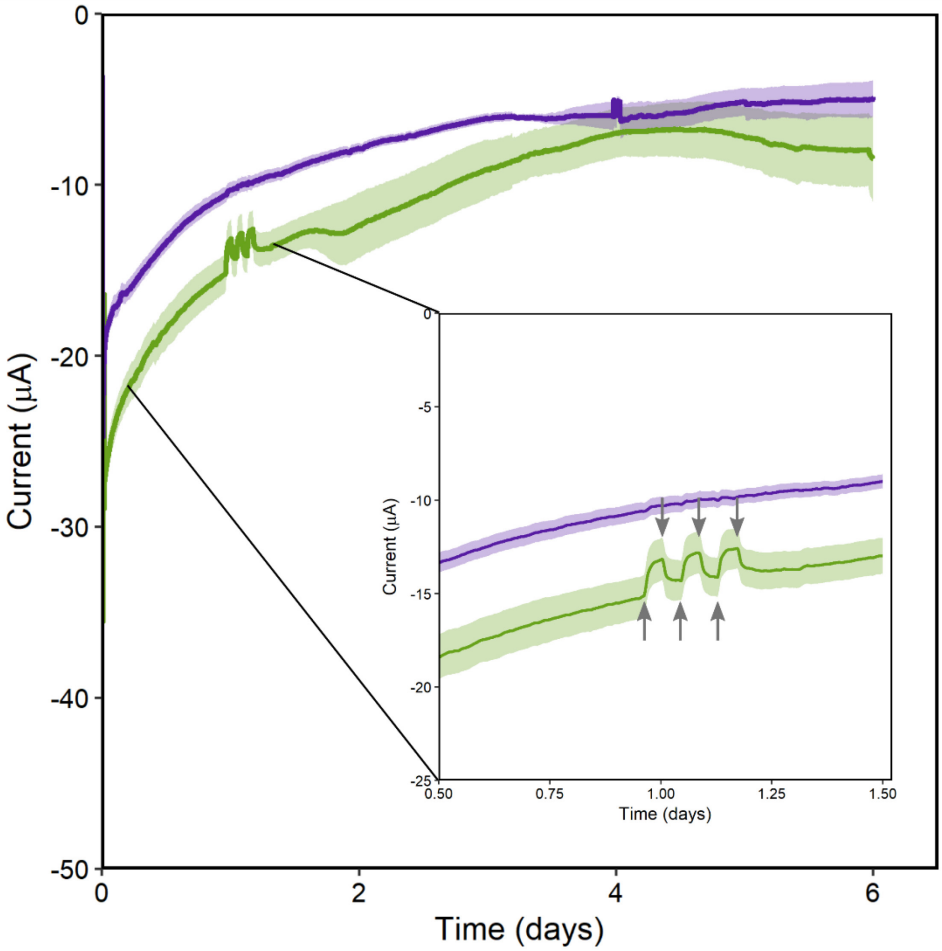

Figure 3. Response of cathodic current to green light. Current was measured in bioelectrochemical systems with electrodes poised at -0.3 V_{SHE}. Current shown was measured beginning at injection of acetoin (time 0). Current measured in reactors containing cells with holo-PR are shown in green and those containing apo-PR are shown in purple. Inset graph shows current change due to removal or addition of green light. Lights were turned off for 3 one hour intervals beginning just before time = 1 day. Each line represents the average of three replicates with standard error shown in transparent ribbons.

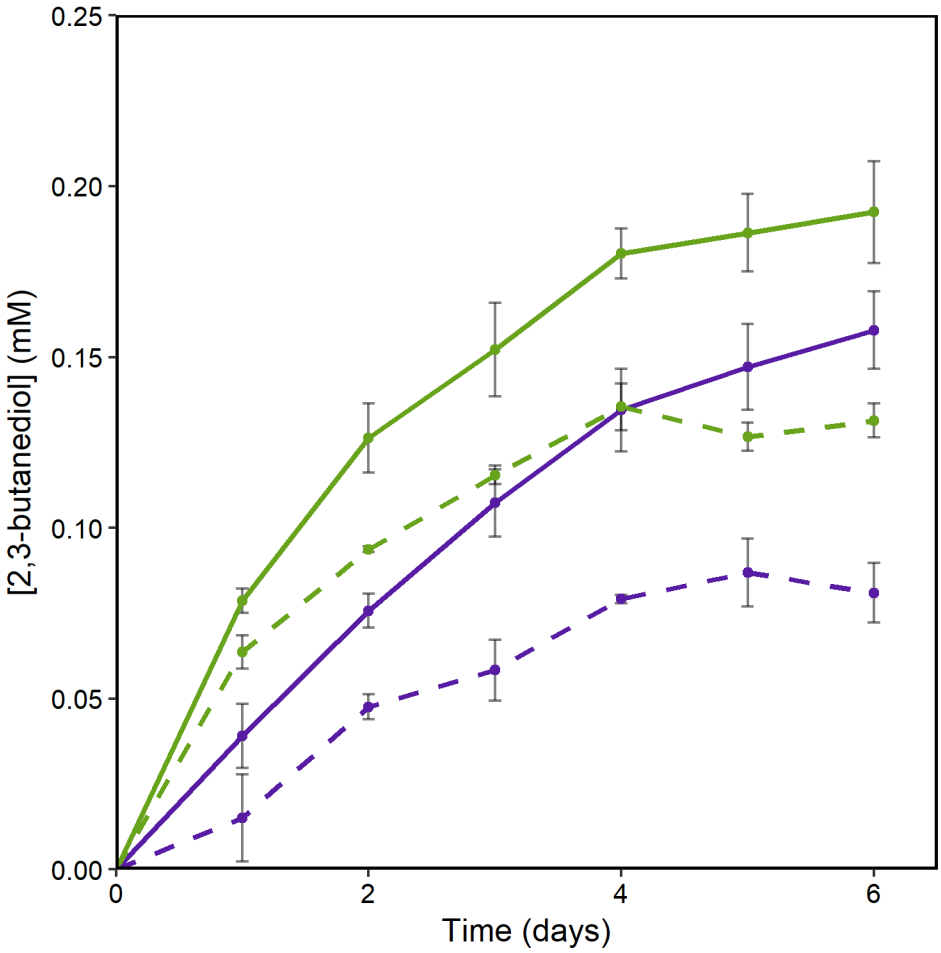

Figure 4. 2,3-butanediol accumulation increases when potential is applied to the working electrode. HPLC measurement of 2,3 butanediol concentration in bioelectrochemical systems over time. Samples taken from working electrode chambers with electrodes poised at -0.3 V_{SHE} are shown in solid green and purple lines. Samples taken from bioelectrochemical systems disconnected from the potentiostat are shown in dashed green and purple lines. Samples from reactors containing cells with holo-PR are shown in green and those containing apo-PR are shown in purple. Each point represents the average of three replicates with standard error shown in error bars.

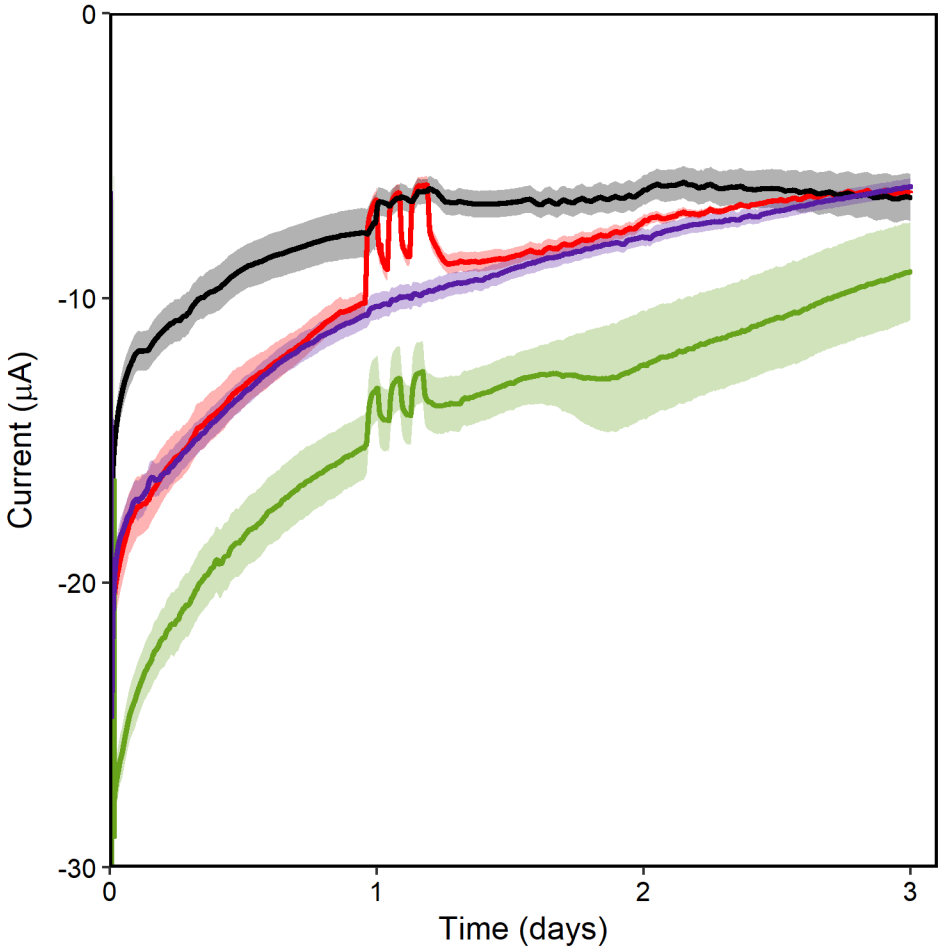

Figure 5. Both proteorhodopsin and butanediol dehydrogenase increase current. Current measured in bioelectrochemical systems containing cells expressing Bdh-PR with holo-PR are shown in green and those containing apo-PR are shown in purple. Current measured in reactors containing cells expressing only holo-PR are shown in red and those containing only apo-PR are shown in black. Current was measured in bioreactors with electrodes poised at -0.3 V_{SHE}. Current shown begins at injection of acetoin (time 0). Each line represents the average of three replicates with standard error shown in transparent ribbons.

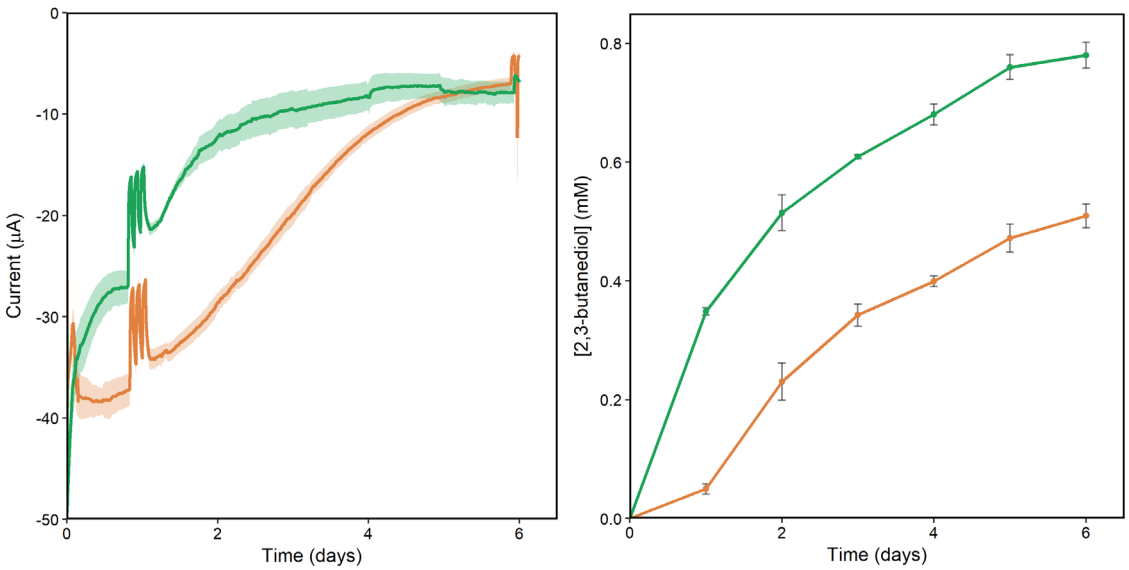

Figure 6. Removal of native hydrogenases decreases current and increases 2,3-butanediol production. (A) Current and (B) 2,3-butanediol accumulation observed in bioreactors containing cells expressing Bdh and holo-PR. The strain without hydrogenases is shown in dark green and the wild-type background is shown in orange. Data shown was measured beginning at injection of acetoin (time 0). Each point represents the average of three replicates with standard error shown in transparent ribbons or error bars.

References

1. **Rabaey K**, **Rozendal RA**. 2010. Microbial electrosynthesis — revisiting the electrical route for microbial production. Nat Rev Microbiol **8**:706–716.
2. **Rosenbaum MA**, **Henrich AW**. 2014. Engineering microbial electrocatalysis for chemical and fuel production. Curr Opin Biotechnol **29**:93–98.
3. **Nevin KP**, **Woodard TL**, **Franks AE**, **Summers ZM**, **Lovley DR**. 2010. Microbial electrosynthesis: Feeding microbes electricity to convert carbon dioxide and water to multicarbon extracellular organic compounds. MBio **1**:e00103-10.
4. **Nevin KP**, **Hensley SA**, **Franks AE**, **Summers ZM**, **Ou J**, **Woodard TL**, **Snoeyenbos-West OL**, **Lovley DR**. 2011. Electrosynthesis of organic compounds from carbon dioxide is catalyzed by a diversity of acetogenic microorganisms. Appl Environ Microbiol **77**:2882–2886.
5. **Ganigué R**, **Puig S**, **Batlle-Vilanova P**, **Balaguer MD**, **Colprim J**, **Mikkelsen M**, **Jørgensen M**, **Krebs FC**, **Haszeldine RS**, **Rabaey K**, **Rozendal RA**, **Nevin KP**, **Woodard TL**, **Franks AE**, **Summers ZM**, **Lovley DR**, **Marshall CW**, **Ross DE**, **Fichot EB**, **Norman RS**, **May HD**, **Marshall CW**, **Ross DE**, **Fichot EB**, **Norman RS**, **May HD**, **Sharma M**, **Aryal N**, **Sarma PM**, **Vanbroekhoven K**, **Lal B**, **Benetton XD**, **Pant D**, **Steinbusch KJJ**, **Hamelers HVM**, **Schaap JD**, **Kampman C**, **Buisman CJN**, **Eerten-Jansen MCAA Van**, **Heijne A Ter**, **Grootscholten TIM**, **Steinbusch KJJ**, **Sleutels THJA**, **Hamelers HVM**, **Buisman CJN**, **Dwidar M**, **Park J-Y**, **Mitchell RJ**, **Sang B-I**, **Sánchez P**, **Ganigue R**, **Bañeras L**, **Colprim J**, **Daniell J**, **Köpke M**, **Simpson SD**, **Gössner AS**, **Picardal F**, **Tanner RS**, **Drake HL**, **Thauer RK**, **Jungermann K**, **Decker K**, **Pi PPH**, **Agler MT**, **Wrenn BA**, **Zinder SH**, **Angenent LT**, **Batlle-Vilanova P**, **Puig S**, **Gonzalez-Olmos R**, **Vilajeliu-Pons A**, **Bañeras L**, **Balaguer MD**, **Colprim J**, **Jeremiasse AW**, **Hamelers HVM**, **Buisman CJN**, **Eerten-jansen MCAA Van**, **Heijne A Ter**, **Buisman CJN**, **Hamelers HVM**, **Bechthold I**, **Bretz K**, **Kabasci S**, **Kopitzky R**, **Springer A**, **Andersen SJ**, **Hennebel T**, **Gildemyn S**, **Coma M**, **Desloover J**, **Berton J**, **Tsukamoto J**, **Stevens C V.**, **Rabaey K**, **Tanner RS**, **Miller LM**, **Yang D**. 2015. Microbial electrosynthesis of butyrate from carbon dioxide. Chem Commun **51**:3235–3238.
6. **Patil SA**, **Arends JBA**, **Vanwonterghem I**, **van Meerbergen J**, **Guo K**, **Tyson GW**, **Rabaey K**. 2015. Selective enrichment establishes a stable performing community for microbial electrosynthesis of acetate from CO_2. Environ Sci Technol **49**:8833–8843.
7. **Park DH**, **Zeikus JG**. 1999. Utilization of electrically reduced neutral red by *Actinobacillus succinogenes*: Physiological function of neutral red in membrane-driven fumarate reduction and energy conservation. J Bacteriol **181**:2403–2410.
8. **Park DH**, **Laivenieks M**, **Guettler M V**, **Jain MK**, **Zeikus JG**. 1999. Microbial utilization of electrically reduced neutral red as the sole electron donor for growth and metabolite production. Appl Environ Microbiol **65**:2912–7.
9. **Drake HL**, **Gößner AS**, **Daniel SL**. 2008. Old acetogens, new light, p. 100–128. *In* Annals of the New York Academy of Sciences.
10. **Müller V**. 2003. Energy Conservation in Acetogenic Bacteria. Appl Environ Microbiol.
11. **Ueki T**, **Nevin KP**, **Woodard TL**, **Lovley DR**. 2014. Converting carbon dioxide to butyrate with an engineered strain of Clostridium ljungdahlii. MBio **5**.
12. **Schiel-Bengelsdorf B**, **Dürre P**. 2012. Pathway engineering and synthetic biology using acetogens. FEBS Lett **586**:2191–2198.

13. **Harrington TD**, **Tran VN**, **Mohamed A**, **Renslow R**, **Biria S**, **Orfe L**, **Call DR**, **Beyenal H**. 2015. The mechanism of neutral red-mediated microbial electrosynthesis in *Escherichia coli*: menaquinone reduction. Bioresour Technol **192**:689–95.
14. **Harrington TD**, **Mohamed A**, **Tran VN**, **Biria S**, **Gargouri M**, **Park J-J**, **Gang DR**, **Beyenal H**. 2015. Neutral red-mediated microbial electrosynthesis by *Escherichia coli, Klebsiella pneumoniae,* and *Zymomonas mobilis*. Bioresour Technol **195**:57–65.
15. **Le QAT**, **Kim HG**, **Kim YH**. 2018. Electrochemical synthesis of formic acid from CO2 catalyzed by Shewanella oneidensis MR-1 whole-cell biocatalyst. Enzyme Microb Technol **116**:1–5.
16. **Batlle-Vilanova P**, **Puig S**, **Gonzalez-Olmos R**, **Balaguer MD**, **Colprim J**. 2016. Continuous acetate production through microbial electrosynthesis from CO2with microbial mixed culture. J Chem Technol Biotechnol **91**:921–927.
17. **Jourdin L**, **Grieger T**, **Monetti J**, **Flexer V**, **Freguia S**, **Lu Y**, **Chen J**, **Romano M**, **Wallace GG**, **Keller J**. 2015. High acetic acid production rate obtained by microbial electrosynthesis from carbon dioxide. Environ Sci Technol **49**:13566–13574.
18. **Jourdin L**, **Freguia S**, **Flexer V**, **Keller J**. 2016. Bringing high-rate, CO_2-based microbial electrosynthesis closer to practical implementation through improved electrode design and operating conditions. Environ Sci Technol **50**:1982–1989.
19. **Batlle-Vilanova P**, **Ganigué R**, **Ramió-Pujol S**, **Bañeras L**, **Jiménez G**, **Hidalgo M**, **Balaguer MD**, **Colprim J**, **Puig S**. 2017. Microbial electrosynthesis of butyrate from carbon dioxide: Production and extraction. Bioelectrochemistry **117**:57–64.
20. **Bajracharya S**, **ter Heijne A**, **Dominguez Benetton X**, **Vanbroekhoven K**, **Buisman CJN**, **Strik DPBTB**, **Pant D**. 2015. Carbon dioxide reduction by mixed and pure cultures in microbial electrosynthesis using an assembly of graphite felt and stainless steel as a cathode. Bioresour Technol **195**:14–24.
21. **Coursolle D**, **Gralnick JA**. 2012. Reconstruction of extracellular respiratory pathways for iron(III) reduction in *Shewanella oneidensis* strain MR-1. Front Microbiol **3**:56.
22. **Coursolle D**, **Baron DB**, **Bond DR**, **Gralnick JA**. 2010. The Mtr respiratory pathway is essential for reducing flavins and electrodes in *Shewanella oneidensis*. J Bacteriol **192**:467–474.
23. **Clarke TA**, **Edwards MJ**, **Gates AJ**, **Hall A**, **White GF**, **Bradley J**, **Reardon CL**, **Shi L**, **Beliaev AS**, **Marshall MJ**, **Wang Z**, **Watmough NJ**, **Fredrickson JK**, **Zachara JM**, **Butt JN**, **Richardson DJ**. 2011. Structure of a bacterial cell surface decaheme electron conduit. Proc Natl Acad Sci **108**:9384–9389.
24. **Myers CR**, **Myers JM**. 2002. MtrB Is required for proper incorporation of the cytochromes OmcA and OmcB into the outer membrane of *Shewanella putrefaciens* MR-1. Appl Environ Microbiol **68**:5585–5594.
25. **Liu Y**, **Wang Z**, **Liu J**, **Levar C**, **Edwards MJ**, **Babauta JT**, **Kennedy DW**, **Shi Z**, **Beyenal H**, **Bond DR**, **Clarke TA**, **Butt JN**, **Richardson DJ**, **Rosso KM**, **Zachara JM**, **Fredrickson JK**, **Shi L**. 2014. A trans-outer membrane porin-cytochrome protein complex for extracellular electron transfer by *Geobacter sulfurreducens* PCA. Environ Microbiol Rep **6**:776–785.
26. **Marritt SJ**, **Lowe TG**, **Bye J**, **McMillan DGG**, **Shi L**, **Fredrickson J**, **Zachara J**, **Richardson DJ**, **Cheesman MR**, **Jeuken LJC**, **Butt JN**. 2012. A functional description of CymA, an electron-transfer hub supporting anaerobic respiratory flexibility in *Shewanella*. Biochem J **444**:465–474.

564 27. **Fredrickson JK**, **Romine MF**, **Beliaev AS**, **Auchtung JM**, **Driscoll ME**, **Gardner TS**,
565 **Nealson KH**, **Osterman AL**, **Pinchuk G**, **Reed JL**, **Rodionov DA**, **Rodrigues JLM**,
566 **Saffarini DA**, **Serres MH**, **Spormann AM**, **Zhulin IB**, **Tiedje JM**. 2008. Towards
567 environmental systems biology of *Shewanella*. Nat Rev Microbiol **6**:592–603.
568 28. **TerAvest MA**, **Ajo-Franklin CM**. 2015. Transforming exoelectrogens for biotechnology
569 using synthetic biology. Biotechnol Bioeng **113**:687–697.
570 29. **Ross DE**, **Flynn JM**, **Baron DB**, **Gralnick JA**, **Bond DR**. 2011. Towards
571 electrosynthesis in *Shewanella*: Energetics of reversing the Mtr pathway for reductive
572 metabolism. PLoS One **6**:e16649.
573 30. **Rowe AR**, **Rajeev P**, **Jain A**, **Pirbadian S**, **Okamoto A**, **Gralnick JA**, **El-Naggar MY**,
574 **Nealson KH**. 2018. Tracking electron uptake from a cathode into *Shewanella* cells:
575 implications for energy acquisition from solid-substrate electron donors. MBio **9**.
576 31. **Pinchuk GE**, **Hill EA**, **Geydebrekht O V**, **De Ingeniis J**, **Zhang X**, **Osterman A**, **Scott**
577 **JH**, **Reed SB**, **Romine MF**, **Konopka AE**, **Beliaev AS**, **Fredrickson JK**, **Reed JL**.
578 2010. Constraint-based model of *Shewanella oneidensis* MR-1 metabolism: a tool for data
579 analysis and hypothesis generation. PLoS Comput Biol **6**:e1000822.
580 32. **Spero MA**, **Aylward FO**, **Currie CR**, **Donohue TJ**. 2015. Phylogenomic analysis and
581 predicted physiological role of the proton-translocating NADH:quinone oxidoreductase
582 (complex I) across bacteria. MBio **6**:e00389-15-.
583 33. **Johnson ET**, **Baron DB**, **Naranjo B**, **Bond DR**, **Schmidt-Dannert C**, **Gralnick JA**.
584 2010. Enhancement of survival and electricity production in an engineered bacterium by
585 light-driven proton pumping. Appl Environ Microbiol **76**:4123–4129.
586 34. **Hunt KA**, **Flynn JM**, **Naranjo B**, **Shikhare ID**, **Gralnick JA**. 2010. Substrate-level
587 phosphorylation is the primary source of energy conservation during anaerobic respiration
588 of *Shewanella oneidensis* strain MR-1. J Bacteriol **192**:3345–3351.
589 35. **Kreuzer HW**, **Hill EA**, **Moran JJ**, **Bartholomew RA**, **Yang H**, **Hegg EL**. 2014.
590 Contributions of the [NiFe]- and [FeFe]-hydrogenase to H_2 production in *Shewanella*
591 *oneidensis* MR-1 as revealed by isotope ratio analysis of evolved H_2. FEMS Microbiol
592 Lett **352**:18–24.
593 36. **Pinchuk GE**, **Geydebrekht O V.**, **Hill EA**, **Reed JL**, **Konopka AE**, **Beliaev AS**,
594 **Fredrickson JK**. 2011. Pyruvate and lactate metabolism by *Shewanella oneidensis* MR-1
595 under fermentation, oxygen limitation, and fumarate respiration conditions. Appl Environ
596 Microbiol **77**:8234–8240.
597 37. **Blanchet E**, **Duquenne F**, **Rafrafi Y**, **Etcheverry L**, **Erable B**, **Bergel A**. 2015.
598 Importance of the hydrogen route in up-scaling electrosynthesis for microbial CO2
599 reduction. Energy Environ Sci **8**:3731–3744.
600 38. **Deutzmann JS**, **Sahin M**, **Spormann AM**. 2015. Extracellular enzymes facilitate
601 electron uptake in biocorrosion and bioelectrosynthesis. MBio **6**.
602 39. **Meshulam-Simon G**, **Behrens S**, **Choo AD**, **Spormann AM**. 2007. Hydrogen
603 metabolism in *Shewanella oneidensis* MR-1. Appl Environ Microbiol **73**:1153–1165.
604 40. **Jensen HM**, **Albers AE**, **Malley KR**, **Londer YY**, **Cohen BE**, **Helms BA**, **Weigele P**,
605 **Groves JT**, **Ajo-Franklin CM**. 2010. Engineering of a synthetic electron conduit in
606 living cells. Proc Natl Acad Sci **107**:19213–19218.
607 41. **Rowe AR**, **Rajeev P**, **Jain A**, **Pirbadian S**, **Okamotao A**, **Gralnick JA**, **El-Naggar MY**,
608 **Nealson K**. 2017. Tracking electron uptake from a cathode into *Shewanella* cells:
609 implications for generating maintenance energy from solid substrates. bioRxiv.

42. **Pinchuk GE**, **Hill EA**, **Geydebrekht O V.**, **de Ingeniis J**, **Zhang X**, **Osterman A**, **Scott JH**, **Reed SB**, **Romine MF**, **Konopka AE**, **Beliaev AS**, **Fredrickson JK**, **Reed JL**. 2010. Constraint-based model of *Shewanella oneidensis* MR-1 metabolism: A tool for data analysis and hypothesis generation. PLoS Comput Biol **6**:1–8.
43. **Duhl, K. L., Tefft, N. M., & TerAvest MA**. 2018. Shewanella oneidensis MR-1 utilizes both sodium- and proton-pumping NADH dehydrogenases during aerobic growth. Appl Environ Microbiol.
44. **Einhauer A**, **Jungbauer A**. 2001. The FLAG™ peptide, a versatile fusion tag for the purification of recombinant proteins. J Biochem Biophys Methods **49**:455–465.
45. **Salis HM**. 2011. The ribosome binding site calculator. Methods Enzymol **498**:19–42.
46. **De Lorenzo V**, **Herrero M**, **Jakubzik U**, **Timmis KN**. 1990. Mini-Tn5 transposoon derivatives for insertion mutagenesis, promoter probing, and chromosomal insertion of cloned DNA in gram-negative eubacteria. J Bacteriol **172**:6568–6572.
47. **Fuhrman JA**, **Schwalbach MS**, **Stingl U**. 2008. Proteorhodopsins: An array of physiological roles? Nat Rev Microbiol **6**:488–494.
48. **Wickham H**. 2009. ggplot2 Elegant Graphics for Data AnalysisMedia.
49. **Wickham H**. 2007. Reshaping data with the reshape package. J Stat Softw **21**:1–20.
50. **Wickham H**, **Francois R**. 2015. dplyr: A Grammar of Data Manipulation. R Packag version 042 3.
51. **Ulrich J**. 2017. TTR: Technical Trading Rules. R Packag version 023-2.
52. **Saltikov CW**, **Newman DK**. 2003. Genetic identification of a respiratory arsenate reductase. Proc Natl Acad Sci U S A **100**:10983–10988.
53. **Myers CR**, **Nealson KH**. 1988. Bacterial manganese reduction and growth with manganese oxide as the sole electron acceptor. Science **240**:1319–1321.
54. **Meshulam-Simon G**, **Behrens S**, **Choo AD**, **Spormann AM**. 2007. Hydrogen metabolism in Shewanella oneidensis MR-1. Appl Environ Microbiol **73**:1153–1165.
55. **Kreuzer HW**, **Hill EA**, **Moran JJ**, **Bartholomew RA**, **Yang H**, **Hegg EL**. 2014. Contributions of the [NiFe]- and [FeFe]-hydrogenase to H_2 production in Shewanella oneidensis MR-1 as revealed by isotope ratio analysis of evolved H(2). FEMS Microbiol Lett **352**:18–24.
56. **Yazynin SA**, **Deyev SM**, **Jucovič M**, **Hartley RW**. 1996. A plasmid vector with positive selection and directional cloning based on a conditionally lethal gene. Gene **169**:131–132.
57. **Beja O**, **Aravind L**, **Koonin E V.**, **Suzuki MT**, **Hadd A**, **Nguyen LP**, **Jovanovich SB**, **Gates CM**, **Feldman RA**, **Spudich JL**, **Spudich EN**, **DeLong EF**. 2000. Bacterial rhodopsin: Evidence for a new type of phototrophy in the sea. Science.